Journal of Zhejiang University-SCIENCE A (Applied Physics & Engineering)
ISSN 1673-565X (Print); ISSN 1862-1775 (Online)
www.zju.edu.cn/jzus; www.springerlink.com
E-mail: jzus@zju.edu.cn

Simulation of top-down crack propagation in asphalt pavements*

Hui LUO[1,2], Hong-ping ZHU[†‡1,2], Yu MIAO[1,2], Chuan-yao CHEN[1,2]

([1]*School of Civil Engineering and Mechanics, Huazhong University of Science and Technology, Wuhan 430074, China*)

([2]*Hubei Key Laboratory of Control Structure, Huazhong University of Science and Technology, Wuhan 430074, China*)

[†]E-mail: hpzhu@mail.hust.edu.cn

Received Apr. 30, 2009; Revision accepted July 5, 2009; Crosschecked Jan. 6, 2010

Abstract: Top-down crack in asphalt pavements has been reported as a widespread mode of failure. A solid understanding of the mechanisms of crack growth is essential to predict pavement performance in the context of thickness design, as well as in the design and optimization of mixtures. Using the coupled element free Galerkin (EFG) and finite element (FE) method, top-down crack propagation in asphalt pavements is numerically simulated on the basis of fracture mechanics. A parametric study is conducted to isolate the effects of overlay thickness and stiffness, base thickness and stiffness on top-down crack propagation in asphalt pavements. The results show that longitudinal wheel loads are disadvantageous to top-down crack because it increases the compound stress intensity factor (SIF) at the tip of top-down crack and shortens the crack path, and thus the fatigue life descends. The SIF experiences a process "sharply ascending—slowly descending—slowly ascending—sharply ascending again" with the crack propagating. The thicker the overlay or the base, the lower the SIF; the greater the overlay stiffness, the higher the SIF. The crack path is hardly affected by stiffness of the overlay and base.

Key words: Road engineering, Top-down crack, Coupled element free Galerkin (EFG) and finite element (FE) method, Stress intensity factor (SIF), Crack propagating path

doi:10.1631/jzus.A0900248 **Document code:** A **CLC number:** TU3

1 Introduction

Cracking is one of the most influential distresses that govern the service life of asphalt concrete pavements. Since cracking leads to water penetration, thereby weakening the foundation of the pavement structure and contributing to increased roughness, a number of studies have been conducted to obtain a better understanding of cracking mechanisms in asphalt concrete pavements (Myers *et al*., 2001; de Freitas *et al*., 2005). A solid understanding of the mechanisms of crack growth is essential to predict pavement performance in the context of thickness design, as well as in the design and optimization of mixtures. Top-down crack in asphalt pavements has been reported as a widespread mode of failure. Recently, most studies on top-down crack of asphalt pavements have focused on the initiation (Svasdisant *et al*., 2002; Wang *et al*., 2003), but the mechanisms for top-down crack propagation have not been completely explained, only little literature involved (Sangpetngam *et al*., 2004; Mao *et al*., 2004).

The theory of fracture mechanics has been used as a basis for predicting crack growth in asphalt mixtures. But the complexity of the problem and the lack of simple-to-use analysis tools have been obstacles to a better understanding of hot-mix asphalt fracture mechanics. Until today, the well-known finite element (FE) method has been the primary tool used for modeling cracks and their effects in mixtures and pavements (Song *et al*., 2006). Unfortunately, it is both complex and numerically intensive for fracture mechanics applications. Some researchers predicted crack growth in asphalt mixtures with the boundary element method (BEM) (Sangpetngam *et al*., 2004), but the BEM is not capable of dealing with the

‡ Corresponding author

* Project (Nos. 50908093 and 50778077) supported by the National Natural Science Foundation of China

multi-medium issues and complicated nonlinear problems.

The element free Galerkin (EFG) method is advantageous in solving moving boundary problems, such as modeling of growing cracks. Fundamentally in EFG, a structured mesh is not used, since only a scattered set of nodal points is required in the domain of interest. This feature presents significant implications for modeling fracture propagation, because the domain of interest is completely discretized by a set of nodes. Since no element connectivity data are needed, the burdensome remeshing required by the FE method can be avoided.

Although EFG is attractive for simulating crack propagation, it costs more computational time than a regular FE, and the imposition of the essential boundary conditions is complicated. Furthermore, due to the level of maturity and comprehensive capabilities of FE, it is often advantageous to use EFG only in the sub-domains where its capabilities can be exploited efficiently.

In this work, a combination of coupled EFG and FE modeling and fracture mechanics was selected for physical representation and analysis of a pavement with a growing top-down crack, and the effect on the crack propagation of structural parameters was analyzed.

2 Numerical theories

2.1 Element free Galerkin method

The EFG method adopts the moving least-squares (MLS) to construct the approximate function (Belytschko *et al*., 1994; 1995; 1996)

$$u^h(x)=\Phi(x)\bar{\boldsymbol{u}}, \tag{1}$$

where $u^h(x)$ is the approximate function, $\bar{\boldsymbol{u}}=(u_1,u_2,\ldots,u_n)^{\mathrm{T}}$ is the parameter vector about nodes, and $\Phi(x)$ is the MLS shape function which could be written as

$$\boldsymbol{\Phi}(x)=[\Phi_1(x),\ \Phi_2(x),\ \ldots,\ \Phi_n(x)]=\boldsymbol{P}^{\mathrm{T}}(x)\boldsymbol{A}^{-1}(x)\boldsymbol{B}(x), \tag{2}$$

where

$$\boldsymbol{A}(x)=\boldsymbol{P}^{\mathrm{T}}(x)\boldsymbol{W}(x)\boldsymbol{P}(x), \tag{3}$$

$$\boldsymbol{B}(x)=\boldsymbol{P}^{\mathrm{T}}(x)\boldsymbol{W}(x). \tag{4}$$

The matrices $\boldsymbol{P}(x)$ and $\boldsymbol{W}(x)$ are defined as

$$\boldsymbol{P}(x)=\begin{bmatrix} p_1(x_1) & p_2(x_1) & \cdots & p_m(x_1)\\ p_1(x_2) & p_2(x_2) & \cdots & p_m(x_2)\\ \vdots & \vdots & & \vdots\\ p_1(x_n) & p_2(x_n) & \cdots & p_m(x_n)\end{bmatrix}, \tag{5}$$

$$\boldsymbol{W}(x)=\begin{bmatrix} w(x-x_1) & 0 & \ldots & 0\\ 0 & w(x-x_2) & \ldots & 0\\ \vdots & \vdots & & \vdots\\ 0 & 0 & \cdots & w(x-x_n)\end{bmatrix}, \tag{6}$$

where $\boldsymbol{p}(x)=[p_1(x),\ p_2(x),\ \ldots,\ p_m(x)]$ is the basis function, and m is the order of the basis function; $w(x-x_i)$ is the weight function associated with node i. In this study, a linear basic function and cubic spline weight function are chosen.

2.2 Coupled element free Galerkin and finite element method

A domain of problem with a hybrid discretization between FE and EFG particles was illustrated in Fig. 1 (Belytschko *et al*., 1995). The superscripts FE and EFG indicate the domain for the FE and EFG particles, respectively. The transition region is designated by Ω^{B}, Ω^{EFG} denotes the EFG domain and Ω^{FE} is the FE domain. The FE and EFG particle boundaries are Γ^{FE} and Γ^{EFG}, respectively. In the interface region, an approximation is given by

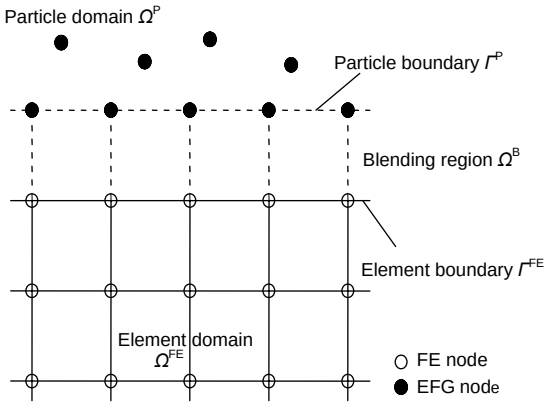

Fig. 1 Discretization of the coupled EFG and FE method (Belytschko *et al*., 1995)

$$u^h(x)=u^{\mathrm{FE}}(x)+R(x)(u^{\mathrm{EFG}}(x)-u^{\mathrm{FE}}(x)),\ x\in\Omega^{\mathrm{B}}, \quad (7)$$

where $u^{\mathrm{FE}}(x)$ and $u^{\mathrm{EFG}}(x)$ are the FE and EFG particle approximations for $u(x)$ in the transition region, respectively, and $R(x)$ is a ramp function, so $R(x)=1$, $x\in\Gamma^{\mathrm{EFG}}$ and $R(x)=0$, $x\in\Gamma^{\mathrm{FE}}$. It is constructed with the use of a linear function along the interface element boundaries so that continuity is ensured (Rabczuk *et al*., 2006):

$$R(x)=3r^2(x)-2r^3(x), \quad (8)$$

with

$$r(x)=\sum_{J\in S_{\Gamma^{\mathrm{EFG}}}} N_J(x), \quad (9)$$

where $S_{\Gamma^{\mathrm{EFG}}}$ is the set of nodes on Γ^{EFG}, and $N_J(x)$ is a shape function of FE. Substituting the FE approximations and the EFG approximations into Eq. (7), the approximation in the transition region is obtained:

$$u^h(x)=\sum_I \tilde{\Phi}_I(x)d_I,\ x_I\in\Omega^{\mathrm{B}}, \quad (10)$$

with the interface shape function

$$\begin{cases}\tilde{\Phi}_I(x)=(1-R(x))N_I(\xi(x))+R(x)\Phi_I(x), \\ \qquad x\in\Omega^{\mathrm{B}}, \\ \tilde{\Phi}_I(x)=R(x)\Phi_I(x),\ x\notin\Omega^{\mathrm{B}},\end{cases} \quad (11)$$

where $\xi(x)$ is the isoparametric coordinate of FE.

3 Computational fracture mechanics

Yang *et al*. (1996) calculated stress intensity factors (SIFs) using a contour integral method. The method is not only fit for mode-I crack, but also fit for mix-mode crack. In this study, we use this method for the calculation of SIF.

Based on linear elastic fracture mechanics, the maximum circumferential tensile stress criterion is used for the simulation of crack propagation (Erdogan and Sih, 1963). The theory has two hypotheses: (1) the crack propagates along the direction where circumferential tensile stress is maximal; (2) the crack starts to propagate while the SIF along the direction is equal to or greater than the critical value K_{IC}.

$$\begin{cases}\theta_0=-\arctan\dfrac{3K_{\mathrm{II}}}{K_{\mathrm{I}}}+\arcsin\dfrac{K_{\mathrm{II}}}{\sqrt{K_{\mathrm{I}}^2+3K_{\mathrm{II}}^2}}, \\ \dfrac{1}{2}\cos\dfrac{\theta}{2}\left[K_{\mathrm{I}}(1+\cos\theta)-3K_{\mathrm{II}}\sin\theta\right]=K_{\mathrm{IC}},\end{cases} \quad (12)$$

where K_{I} and K_{II} are SIFs of mode-I and mode-II, respectively, θ_0 is the direction of crack propagation, and K_{IC} is the fracture toughness.

Crack propagation is a nonlinear dynamic continuous process. To simulate it, the process is divided into a lot of successive increments. In each increment, crack propagation will be considered to be a quasi-static problem. Thus, during every increment, the variation of stress field at crack tip is neglectable, and the crack propagates along a straight line. The selection of the length of the increment has a direct impact on the success of the simulation. If the length is too large, it will lead to large errors which cause the simulation to deviate from the actual situation; if the length selected is too small, although it helps to improve the accuracy, it will greatly reduce the computational efficiency. Based on experience, about 1/20−1/10 of the initial crack length is recommended as the incremental length.

After every crack propagating increment, the original node at crack tip should be split into two nodal points, and a new crack-tip node will be created. The distance between the new and old crack-tip nodes is equal to the incremental length da (Fig. 2).

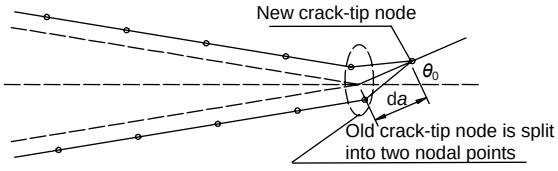

Fig. 2 The crack structure change after a propagating increment

4 Fatigue life prediction

Paris and Erdogan (1965) indicated that the fatigue crack growth rate is a power function of the SIF at crack tip

$$\frac{\mathrm{d}a}{\mathrm{d}N} = A[\Delta K(a)]^n, \tag{13}$$

where a is the crack length, N is the number of cyclic loads, ΔK is the range of SIF at crack tip varied with load cycle, and A and n are material constants.

Eq. (13) is usually called the Paris power law. It can well describe the propagation of top-down crack in asphalt pavements. Furthermore, the format of Paris' power law is simple, which makes it easily understood and promoted into use. By integrating Paris' power law, the fatigue life of the crack propagation is available:

$$N_\mathrm{f} = \int_{a_\mathrm{i}}^{a_\mathrm{f}} \frac{\mathrm{d}a}{A[\Delta K(a)]^n}, \tag{14}$$

where a_i is the initial length of crack, a_f is the finial crack length after failure, and N_f is the fatigue life.

For asphalt mixture used in this study, the material constant for the crack growth rate is referred to Jacobs (1995), where A and n are 3.44×10^{-6} and 2.71, respectively.

As shown in Eq. (14), to obtain the fatigue life N_f, the SIF at crack tip must be solved. This could be done using the method described in Section 3.

5 Numerical model for top-down crack propagation in asphalt pavement

In a certain range region near the wheel loads, asphalt overlay surface is in compression, and out of this region, asphalt overlay surface is in tension, and the site where maximum tensile stress starts is correlated to asphalt pavement structure (Myers *et al*., 2001). In this study, referring to Mao *et al*. (2004), the wheel load is 450 mm horizontally away from the crack. The schematic is shown in Fig. 3. The initial length of top-down crack is 40 mm; the wheel loads include two portions: the vertical part p is 0.7 MPa, and the longitudinal one τ is 30% of the vertical, according to Siddharthan *et al*. (1998). Fig. 3b is the numerical discretization of the coupled EFG and FE. The two sides of the mesh were fixed horizontally but allowed to displace vertically, whereas the bottom was assumed rough by restraining horizontally and displacing vertically. The parameters of the pavement structure are shown in Table 1 (Mao *et al*., 2004).

Table 1 The structure parameters of the pavement (Mao *et al*., 2004)*

Layer	Thickness (mm)	Young's modulus (MPa)	Poisson's ratio
Asphalt overlay	160	2000	0.25
Base	200	1000	0.25
Bottom base	200	500	0.25
Sub-grade	1000	50	0.35

* Initial crack lengths of all the layers are 40 mm

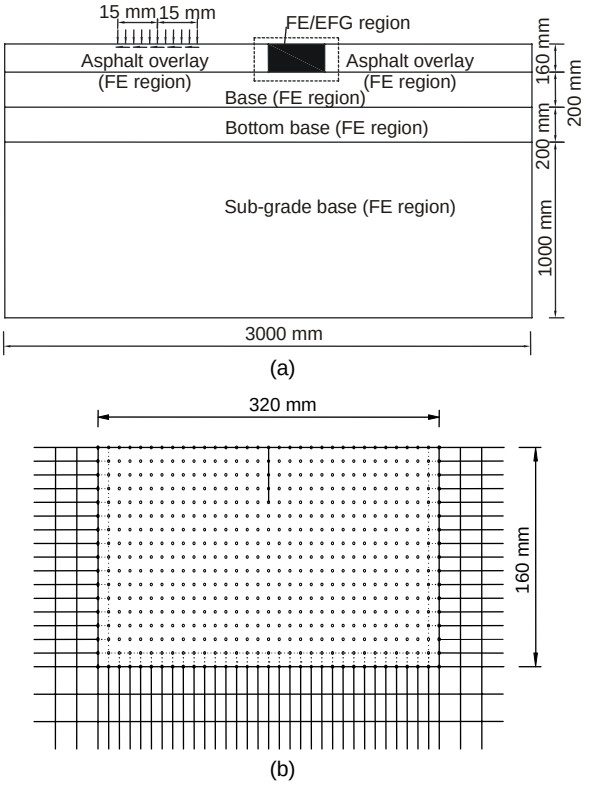

Fig. 3 The numerical discretization of the pavement
(a) Global numerical discretization; (b) Detail of top-down crack region

6 Results and discussion

A parametric study is conducted to isolate the effects of various parameters on top-down crack propagation. The parameters evaluated include: wheel load, asphalt overlay thickness, base thickness, overlay stiffness and base thickness.

6.1 Effect of wheel load

Two wheel load cases are conducted in this simulation. Load case 1 is vertical load only, while

load case 2 includes both vertical and longitudinal loads. For simplicity, considering that compound SIF includes both mode-I and mode-II cracking information, only compound SIFs are discussed. The fatigue life is defined as the total number of cyclic loads that drive top-down crack propagating from initial depth till overlay bottom. The results are shown in Fig. 4.

Fig. 4a shows how the compound SIF changes with top-down crack propagation. The SIF-crack length curves are of similar shape. The SIF of case 2 is about 2 MPa·mm$^{1/2}$ greater than that of case 1, and it could be seen that the SIF experiences a process "sharply ascending—slowly descending—slowly ascending—sharply ascending again" as top-down crack propagating. Fig. 4b reveals the paths of the two load cases. It could be found that the path of case 1 deviates horizontally greater than that of case 2. Greater horizontal deviation means longer crack propagating path length, which benefits the fatigue life. Fig. 4c shows the fatigue life of top-down cracks. After considering longitudinal wheel load, the fatigue life is shortened to half of case 1. Fig. 4 illustrates that load case 2 is more disadvantageous, and the sequential analyses adopt load case 2 for security.

6.2 Effect of asphalt overlay thickness

In this case, how overlay thickness affects on top-down crack propagation is studied. In the simulation, overlay thickness varies from 120 mm to 200 mm at the interval of 20 mm. The results are shown in Fig. 5.

Fig. 5a shows that the thicker the asphalt overlay, the smaller the compound SIF. The SIF of a thinner overlay is greater than that of the thicker one at the same crack depth all the time while top-down crack propagating downwards. Fig. 5b reveals top-down crack propagating paths. It appears that overlay thickness has little effect on top-down cracking path. Fig. 5c shows that the fatigue life extends with the increment of overlay thickness. But, when overlay

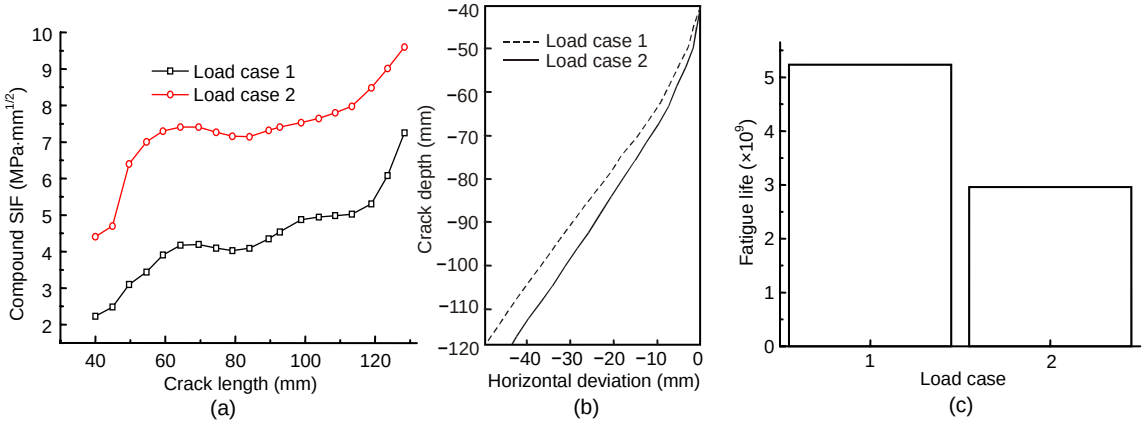

Fig. 4 Effects of load cases on (a) compound SIFs, (b) crack paths and (c) fatigue life

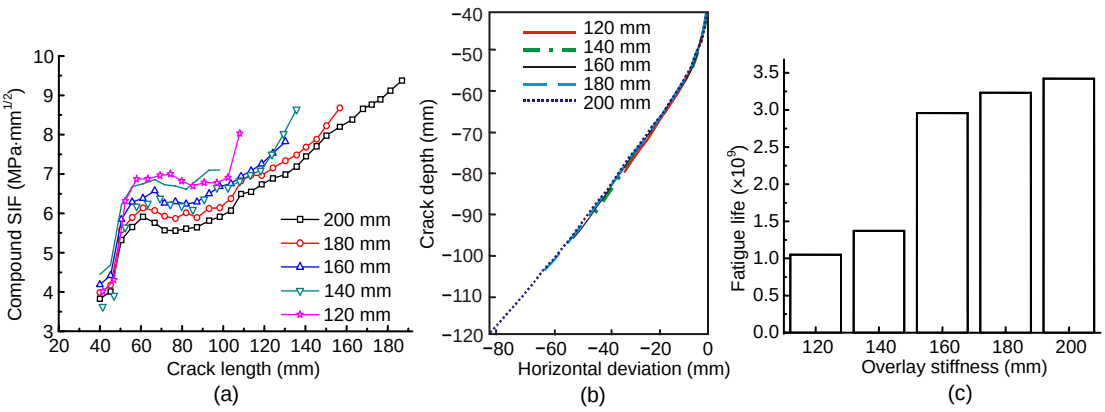

Fig. 5 Effects of overlay thickness on (a) compound SIFs, (b) crack paths and (c) fatigue life

thickness is beyond a certain value, the fatigue life shows no obvious increase. This is to say, it is not appropriate to prolong the pavement service life only by adding overlay thickness.

6.3 Effect of asphalt overlay stiffness

The effect of overlay stiffness on top-down crack propagation is studied in this case. In the simulation work, overlay stiffness varies from 1000 MPa to 4000 MPa at the interval of 1000 MPa. The results are shown in Fig. 6.

Fig. 6a shows that, the stiffer the overlay, the greater the SIF. This may be due to the fact that stiffer overlay bears much more wheel loads, which makes overlay's stress field more disadvantageous. Fig. 6b reveals the crack paths. It could be found that there is a slight variation in paths while overlay stiffness changing; that is, the stiffer the overlay is, the more the crack path horizontally deviates. Fig. 6c shows that the fatigue life descends with the increase of overlay stiffness. This is due to greater compound SIF at the crack tip induced by greater overlay stiffness.

6.4 Effect of base thickness

In this case, how base thickness affects on top-down crack propagation is investigated. In the simulation, base thickness varies from 200 mm to 350 mm at the interval of 50 mm. The results are shown in Fig. 7.

Fig. 7a shows that, the thicker the base, the smaller the compound SIF. The SIF of a thinner base is greater than that of the thicker one at the same crack depth all the time. Fig. 7b reveals that the path deviates slightly more horizontally with the descent of base thickness. Fig. 7c shows that the fatigue life extends with the increment of base thickness.

6.5 Effect of overlay stiffness

The effect of the base stiffness on top-down crack propagation is studied in this case. In the simulation work, base stiffness varies from 1000 MPa to 4000 MPa at the interval of 1000 MPa. The results are shown in Fig. 8.

Fig. 8a shows that greater base stiffness causes

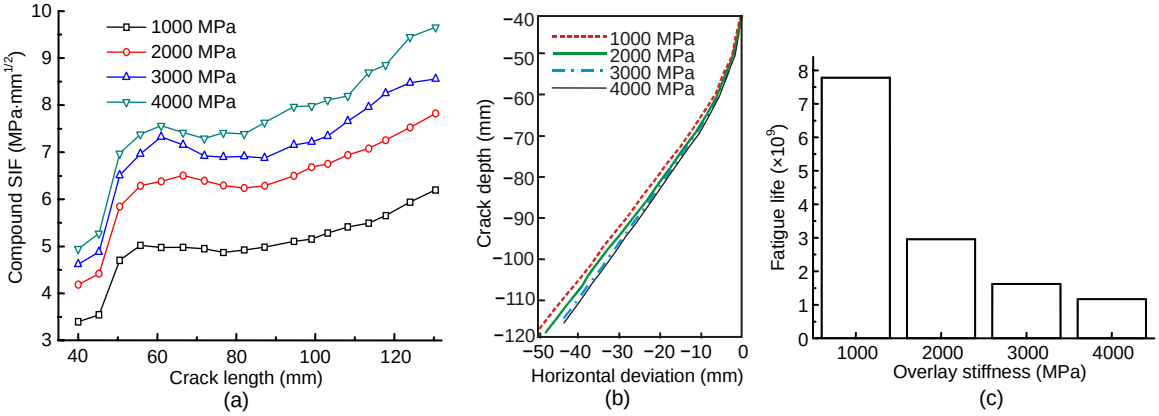

Fig. 6 Effects of overlay stiffness on (a) compound SIFs, (b) crack paths and (c) fatigue life

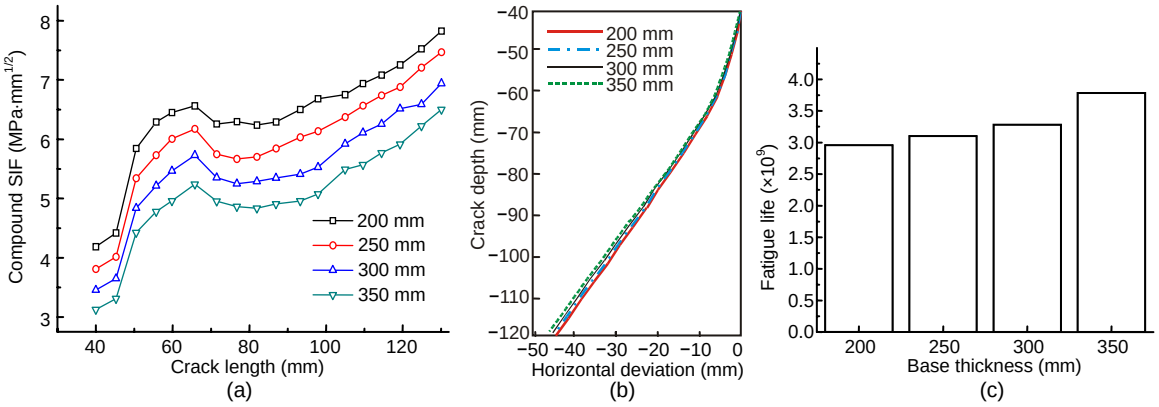

Fig. 7 Effects of base thickness on (a) compound SIFs, (b) crack paths and (c) fatigue life

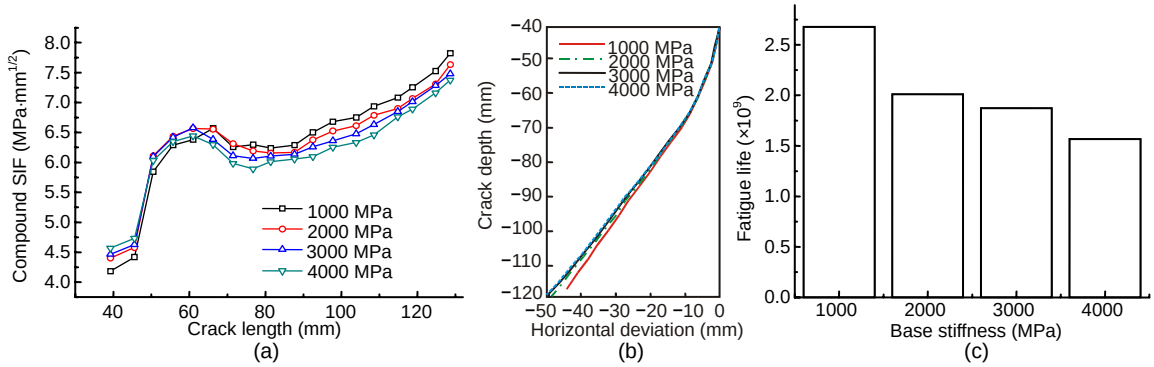

Fig. 8 Effects of base stiffness on (a) compound SIFs, (b) crack paths and (c) fatigue life

higher compound SIF when top-crack is shallow (40 mm−60 mm in this study). If top-down crack propagates deep enough, greater base stiffness leads to lower compound SIF. There exists a conversion between base stiffness and the SIF, depending on the crack depth. Fig. 8b reveals the crack paths. It could be found that the stiffer the base is, the more the crack path horizontally deviates. Fig. 8c shows that the fatigue life descends with the increase of base stiffness.

7 Conclusion

Based on the coupled EFG and FE method which reduces the computational time and simplifies the imposition of the essential boundary conditions of the element free Galerkin (EFG) method, top-down crack propagation in asphalt pavement is simulated, and the parametric study is done to isolate the effect of various parameters on top-down crack propagation. The following conclusions are drawn:

1. Longitudinal wheel load is disadvantageous to the propagation of top-down crack. It aggravates the compound SIF and causes shorter fatigue life.

2. The SIF experiences a process "sharply ascending—slowly descending—slowly ascending—sharply ascending again" as top-down crack propagating.

3. The SIF descends with the increase of overlay thickness and ascends with the increase of overlay stiffness.

4. The crack path is slightly affected by overlay and base stiffness.

References

Belytschko, T., Lu, Y.Y., Gu, L., 1994. Element free Galerkin methods. *International Journal for Numerical Methods in Engineering*, **37**(2):229-256. [doi:10.1002/nme.1620370205]

Belytschko, T., Organ, D., Krongauz, Y., 1995. A coupled finite element-element free Galerkin method. *Computational Mechanics*, **17**(3):186-195. [doi:10.1007/BF00364080]

Belytschko, T., Krongauz, Y., Organ, D., 1996. Meshless methods: an overview and recent developments. *Computer Methods in Applied Mechanics and Engineering*, **139**(1-4):3-47. [doi:10.1016/S0045-7825(96)01078-X]

de Freitas, D., Paulo, P., Luis, P., Thomas, A., 2005. Effect of construction quality, temperature, and rutting on initiation of top-down cracking. *Transportation Research Record, Journal of the Transportation Research Board*, **1929**(1):174-182. [doi:10.3141/1929-21]

Erdogan, F., Sih, G.C., 1963. On the crack extension in plates under plate loading and transverse shear. *Journal of Basic Engineering*, **85**:519-525.

Jacobs, M.M., 1995. Crack Growth in Asphalt Mix. MS Thesis, Delft University of Technology, Delft, Holand.

Mao, C., Qiu, Y.J., Li, Y.P., 2004. Simulation of surface crack propagation in asphalt pavements and analysis of its influential factors. *Journal of Southwest Jiaotong University*, **39**(4):437-441 (in Chinese).

Myers, L.A., Roque, R., Birgisson, B., 2001. Propagation mechanisms for surface-initiated longitudinal wheelpath cracks. *Transportation Research Record Journal of the Transportation Research Board*, **1778**(1):113-122. [doi:10.3141/1778-14]

Paris, P., Erdogan, F., 1963. A critical analysis of crack propagation laws. *Journal of Basic Engineering, Series D*, **85D**(4):528-535.

Rabczuk, T., Xiao, S.P., Sauer, M., 2006. Coupling of mesh-free methods with finite elements: basic concepts and test results. *Communications in Numerical Methods in Engineering*, **22**(10):1031-1065. [doi:10.1002/cnm.871]

Sangpetngam, B., Birgisson, B., Roque, R., 2004. Multilayer boundary-element method for evaluating top-down cracking in hot-mix asphalt pavements. *Transportation Research Record Journal of the Transportation Research Board*, **1896**(1):129-137. [doi:10.3141/1896-13]

Siddharthan, R.V., Yao, J., Sebaaly, P.E., 1998. Pavement

strain from dynamic 3D load distribution. *Journal of Transportation Engineering*, **124**(6):557-566. [doi:10.1061/(ASCE)0733-947X(1998)124:6(557)]

Song, S.H., Paulino, G.H., Buttlar, W.G., 2006. Simulation of crack propagation in asphalt concrete using an intrinsic cohesive zone model. *Journal of Engineering Mechanics*, **132**(11):1215-1223. [doi:10.1061/(ASCE)0733-9399(2006)132:11(1215)]

Svasdisant, T., Schorsch, M., Baladi, G.Y., Pinyosunun, S., 2002. Mechanistic analysis of top-down cracks in asphalt pavements. *Transportation Research Record: Journal of the Transportation Research Board*, **1809**(1):126-136. [doi:10.3141/1809-15]

Wang, L.B., Myers, L.A., Mohammad, L.N., Fu, Y.R., 2003. Micromechanics study on top-down cracking. *Transportation Research Record: Journal of the Transportation Research Board*, **1853**(1):121-133. [doi:10.3141/1853-14]

Yang, X.X., Fan, J.Q., Kuang, Z.B., 1996. A contour integral method for stress intensity factors of mixed-mode crack. *Computational Structural Mechanics and Applications*, **13**(1):84-86 (in Chinese).